Poly(propyleneimine) Liquid Crystal Codendrimers Bearing Laterally and Terminally Attached Promesogenic Groups

Rafael Martín-Rapún,[†] Mercedes Marcos,[†] Ana Omenat,[†] José-Luis Serrano,*[,†] Geoffrey R. Luckhurst,[‡] and Azizah Mainal[‡]

Química Orgánica-Dpto. Nuevos Materiales Orgánicos, Facultad de Ciencias-Instituto de Ciencia de Materiales de Aragón, Universidad de Zaragoza-CSIC, E-50009 Zaragoza, Spain, and School of Chemistry and Southampton Liquid Crystal Institute, University of Southampton, Southampton SO17 1BJ, United Kingdom

Received May 21, 2004. Revised Manuscript Received August 20, 2004

The synthesis, chemical characterization, and liquid crystalline behavior of two new series of poly(propyleneimine) (DAB) codendrimers are described. Both series were obtained by grafting onto the fourth-generation dendrimer (DAB−$(NH_2)_{32}$) various proportions of two types of promesogenic units: one of them laterally attached and the other terminally attached. Both series differ in the terminally attached promesogenic unit, being chiral in series 1 and achiral in series 2. X-ray diffraction studies show that these compounds exhibit nematic or lamellar mesophases. For intermediate proportions, the smectic C mesophase, which was not exhibited by the homodendrimers, appears. Thus, the evolution between a nematic and an orthogonal lamellar mesophase occurs through a tilted mesophase. The chiral centers in series 1 permit the appearance of chiral nematic (N*) and chiral smectic C (SmC*) mesophases, which are studied. Deuterium NMR experiments reveal that the nematic formed by one codendrimer is uniaxial and not the anticipated biaxial nematic.

Introduction

Liquid crystal dendrimers (LCDs) or dendromesogens behave as a specific class in the field of liquid crystal polymers. The functionalization of the terminal reactive groups of dendrimers by means of promesogenic structures allows us to obtain different types of liquid crystal phases.[1−9] In these materials the mesogenic units have stronger restrictions on their mobility, and in many cases the groups are forced to be closer to one another, preventing the microsegregation that is typical of many liquid crystal systems (mixtures). In consequence, dendrimers become an extraordinary tool to study the structure−activity relationships in the liquid crystal field, because they are able to adopt different conformations, provided that the chemical nature of the dendritic core allows for such deformations, to obtain the most stable structures.

Scheme 1. Influence of the Mesogens Topology on the LCD Mesophase

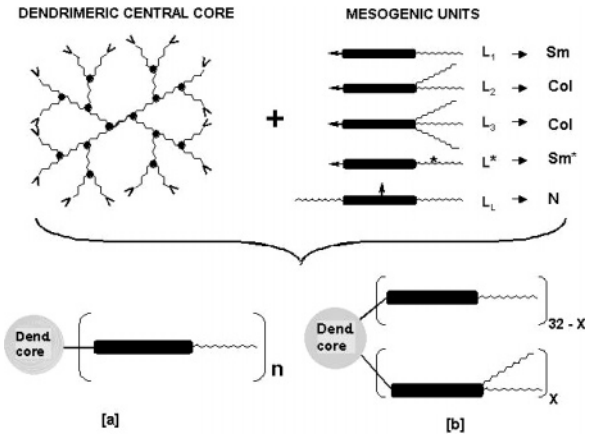

In previous work we have studied several families of homodendrimers and codendrimers functionalized with terminal attached promesogenic units that show calamitic or columnar phases depending on the number of terminal chains (Scheme 1).[10−13] Using codendrimers

* Corresponding author. Fax and phone: (+) 34 976 761209. E-mail: joseluis@unizar.es.
[†] Universidad de Zaragoza-CSIC.
[‡] University of Southampton.

(1) Ponomarenko, S. A.; Boiko, N. I.; Shibaev, V. P. *Polym. Sci. Ser. C* **2001**, *33*, 1−45 and references therein.
(2) Bobrovsky, A.Yu; Pakhomov, A. A.; Zhu, X. M.; Boiko, N. I.; Shibaev, V. P.; Stumpe, J. *J. Phys. Chem. B* **2002**, *106*, 540−546.
(3) Bobrovsky, A. Yu; Ponomarenko, S.; Boiko, N. I.; Shibaev, V.; Rebrov, E.; Muzafarov, A.; Stumpe, J. *J. Macromol. Chem. Phys*. **2002**, *203*, 1539−1546.
(4) Saez, I. M.; Goodby, J. W.; Richardson, R. M. *Chem. Eur. J*. **2001**, *7*, 2758−2764.
(5) Elsässer, R.; Mehl, G. H.; Goodby, J. W.; Veith, M. *Angew. Chem., Int. Ed*. **2001**, *40*, 2688−2690.
(6) Tsiourvas, D.; Stathopoulu, K.; Sideratou, Z.; Paleos, C. M. *Macromolecules* **2002**, *35*, 1746−1750.
(7) Tsiourvas, D.; Felekis, T.; Sideratou, Z.; Paleos, M. C. *Macromolecules* **2002**, *35*, 6466−6469.
(8) Dautlgraber, G.; Baumeister, V.; Diele, S.; Kresse, H.; Luhmann, B.; Lang, H.; Tschierske, C. *J. Am. Chem. Soc*. **2002**, *124*, 14852−14853.
(9) Busson, P.; Örtegren, J.; Ihre, H.; Gedde, U. W.; Hult, A.; Andersson, G.; Eriksson, A.; Lindgren, M. *Macromolecules* **2002**, *35*, 1663−1671.
(10) Barberá, J.; Marcos, M.; Serrano, J. L. *Chem. Eur. J.* **1999**, *5*, 1834−1840.
(11) Marcos, M.; Giménez, R.; Serrano, J. L.; Donnio, B.; Heinrich, B.; Guillon, D. *Chem. Eur. J.* **2001**, *7*, 1006−1013.

10.1021/cm049191l CCC: $27.50
Published on Web 10/27/2004

Scheme 2. Schematic Representation of the Reported Codendrimers[a]

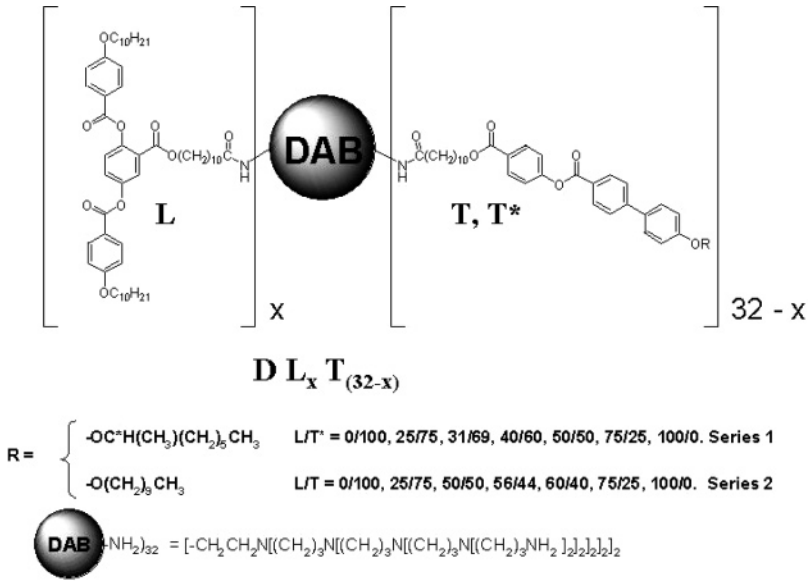

[a] *x* is equal to the number of promesogenic units L.

functionalized with promesogenic units bearing one or two terminal chains it has been possible to follow the gradual transition between calamitic and columnar phases (Scheme 1b).[14] It is also possible to obtain nematic phases in dendrimers functionalized with laterally attached promesogenic units,[4,6,15−19] in a similar way as occurs in side-chain liquid crystal polymers.[20,21]

Recently, one side-on liquid crystalline polymer has been claimed to exhibit a biaxial nematic phase (N_b) on the basis of deuterium NMR experiments.[22] Since the biaxial nematic mesophase was predicted theoretically by Freiser more than 30 years ago,[23] a number of other theoretical investigations have been carried out using various models to predict the possibility of obtaining a N_b liquid crystal.[24] Subsequent experimental work has been reported[24,25] and the N_b mesophase was observed for lyotropic systems and more recently for thermotropic liquid crystals: low molecular weight molecules[26,27] and the aforementioned thermotropic liquid crystal polymers. In the last case, the side-on attachment of the mesogen as a side chain to the polymer is successful in preventing the formation of crystalline and smectic phases and in hindering the rotation about the molecular long axis. Thus, the nematic phase is favored but a cylindrical symmetry (uniaxial) is prevented.

Following our studies in this field we present in this paper the liquid crystal (LC) properties obtained for codendrimers that mix in their structures terminal- and laterally attached promesogenic units. We have synthesized two series of codendrimers using the fourth generation of poly(propyleneimine) (DAB) as a central dendrimeric core (Scheme 2). This dendritic matrix bears 32 terminal amine groups, which can be functionalized via imine or amide bonds. For this work, the latter were chosen due to their higher thermal stability. In both series the laterally attached group L is the same. The mesogenic core of L consists of three aromatic units. The central one derives from 2,5-dihydroxybenzoic acid, and this allows the trisubstitution necessary for the side-on functionalization of the dendrimeric core. This compound bears two decyloxy terminal chains. Moreover, we have introduced two different terminally attached promesogenic cores. They both have the same rigid central core also bearing three aromatic groups and a different terminal tail: the chiral 2-(*R*)-octyloxy in the case of series 1 and decyloxy in the codendrimers of series 2.

In both series the promesogenic units are connected to the DAB central entity by means of a flexible spacer derived from 11-hydroxyundecanoic acid.

Our purpose is three-fold. The first is to study the transition between the nematic (induced by the laterally attached groups[4,5,15]) and the orthogonal smectic phases induced by the terminally attached promesogenic groups[1] as a continuation of our studies on the relationship between structure and liquid crystal properties. Second, we use these codendrimers as a new strategy with which

(12) Barberá, J.; Donnio, B.; Giménez, R.; Guillon, D.; Marcos, M.; Omenat, A.; Serrano, J. L. *J. Mater. Chem.* **2001**, *11*, 2808−2813.
(13) Donnio, B.; Barberá, J.; Giménez, R.; Guillon, D.; Marcos, M.; Serrano, J. L. *Macromolecules* **2002**, *35*, 370−381.
(14) Rueff, J.-M.; Barberá, J.; Donnio, B.; Guillon., D.; Marcos, M.; Serrano, J. L. *Macromolecules* **2003**, *36*, 8368−8375.
(15) Barberá, J.; Giménez, R.; Marcos, M.; Serrano, J. *L. Liq. Cryst.* **2002**, *29*, 309−314.
(16) Mehl, G. H.; Elsässer, R.; Goodby, J. W.; Veith, M. *Mol. Cryst. Liq. Cryst.* **2001**, *364*, 219−224.
(17) Saez, I. M.; Goodby, J. W. *J. Mater. Chem.* **2001**, *11*, 2845−2851.
(18) Campidelli, S.; Eng, C.; Saez, I. M.; Goodby, J. W.; Deschenaux, R. *Chem. Commun.* **2003**, 1520−1521.
(19) Saez, I. M.; Goodby, J. W. *Chem. Eur. J.* **2003**, *9*, 4869−4877.
(20) Hessel, F.; Finkelmann, H. *Polym. Bull.* **1985**, *14*, 375−378.
(21) Keller, P.; Harduin, F.; Mauzac, M.; Achard, M. F. *Mol. Cryst. Liq. Cryst*. **1988**, *155*, 171−178.
(22) Severing, K.; Saalwächter, K. *Phys. Rev. Lett.* **2004**, *92*, 125501−1, 125501−4.
(23) Freiser, M. J. *Phys Rev. Lett.* **1970**, *24*, 1041−1043.
(24) Sadashiva, B. K. *Handbook of Liquid Crystals*; Demus, D., Goodby, J. W., Gray, G. W., Spies, H. W., Vill, V., Eds.; VCH: Weinheim, 1998; Vol. 2A, pp 933−943 and references therein.
(25) Praefcke, K.; Blunk, D.; Singer, D.; Goodby, J. W.; Toyne, K. J.; Hird, M.; Styring, P.; Norbert, W. D. J. A. *Mol. Cryst. Liq. Cryst.* **1998**, *323*, 231−259.
(26) Madsen, L. A.; Dingemans, T. J., Nakata, M.; Samulski, E. T. *Phys. Rev. Lett.* **2004**, *92*, 145505−1, 124505−4.
(27) Acharya, B. R.; Primak, A.; Kumar, S. *Phys. Rev. Lett.* **2004**, *92*, 145506−1, 124506−4.

Scheme 3. Synthetic Route to the Terminally Attached Mesogenic Units T and T* [a]

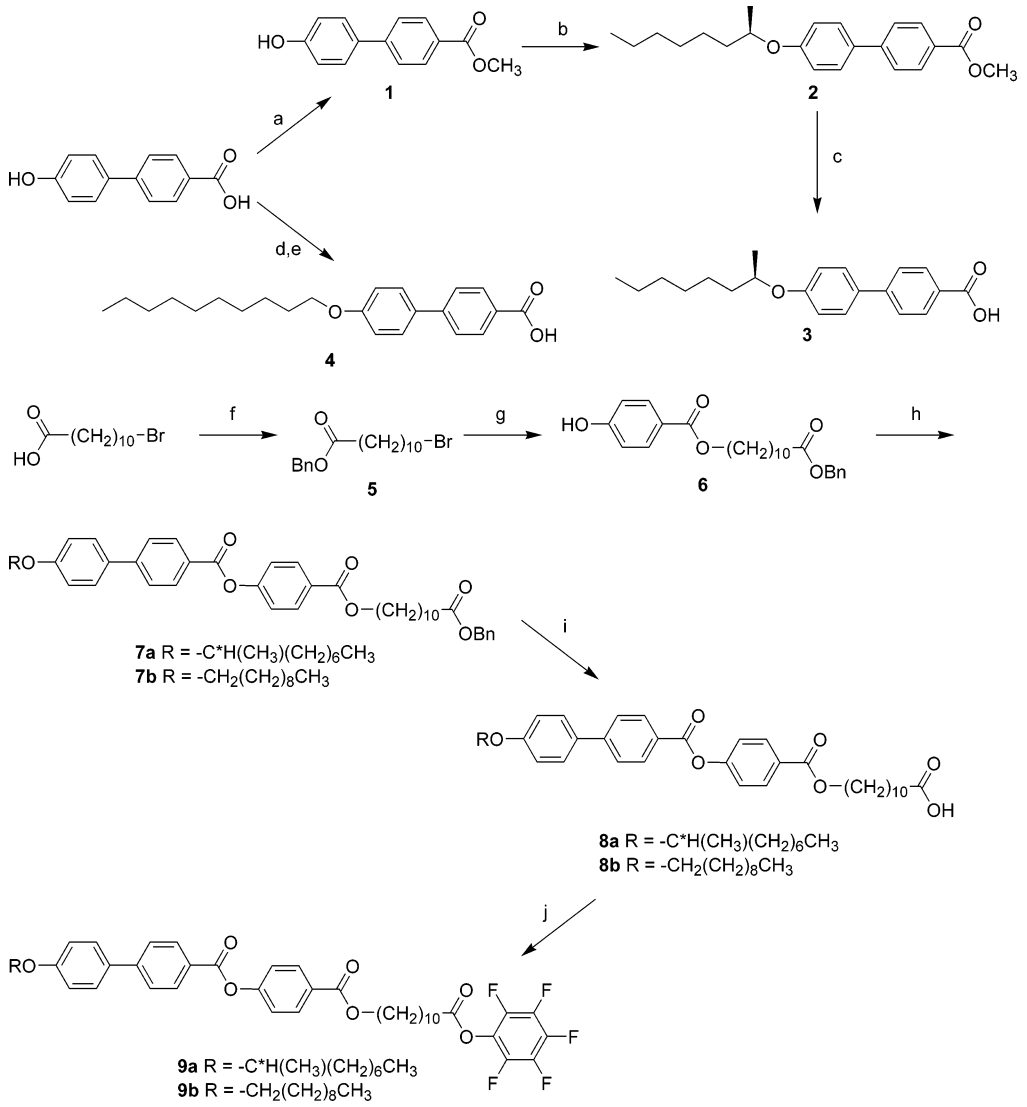

[a] Conditions: (a) H_2SO_4, MeOH; (b) (*S*)-2-octanol, DIAD, TPP, THF;[30] (c) KOH, EtOH; (d) $CH_3(CH_2)_9Br$, KOH (aq), EtOH; (e) KOH/H_2O (10%); (f) BnOH, DCC, DMAP, CH_2Cl_2;[31] (g) $NaHCO_3$, 4-hydroxybenzoic acid, DMF;[32] (h) **3** or **4**, DCC, DMAP, CH_2Cl_2;[31] (i) $Pd(OH)_2/C$ (20%), cyclohexene, THF; (j) C_6F_5OH, DCC, DMAP, CH_2Cl_2.[31]

to obtain biaxial nematic phases taking into account some works reported in the literature. And finally, we try to obtain ferroelectric liquid crystal behavior in series 1, because we expect that these codendrimers will exhibit a smaller viscosity than the dendrimers and codendrimers previously described, which is crucial to allow this behavior.[28]

Results and Discussion

Synthesis. The poly(propyleneimine) dendrimer of the fourth generation was commercially available from Aldrich. The anisotropic units selected for this work were chosen because of the mesogenic behavior of dendrimers functionalized with the same or similar promesogenic units. On one hand, dendrimers with laterally attached calamitic promesogenic units such as L exhibit nematic behavior. On the other hand, the terminally attached calamitic units are well-known to induce a lamellar mesogenic behavior. The promesogenic units were synthesized with a pentafluorophenyl ester as an activating group for the formation of the amide bond, following a synthetic method reported previously.[29]

The synthetic routes to the promesogenic units are based on easy reactions with moderate to high yields. In Scheme 3, the synthesis of the promesogenic units T an T* are presented. The synthesis of promesogenic unit L was performed by a method similar to that previously described by us (Scheme 4).[15]

All dendrimers were functionalized via the nucleophilic attack of the terminal amino groups of the fourth-generation DAB commercial dendrimer on the pentafluorophenyl derivatives **13** and either **9a** or **9b** following a method similar to that described by Meijer et al.[29] DAB−$(NH_2)_{32}$ was introduced in well-defined mixtures of **13** and one of either **9a** or **9b**. As will be seen in the characterization section, the laterally and terminally

(28) Serrano, J. L.; Marcos, M.; Martín, R.; González, M.; Barberá, J. *Chem. Mater.* **2003**, *15*, 3866−3872.

(29) Baars, M. W. P. L.; Söntjens, S. H. M.; Fischer, H. M.; Peerlings, H. W. I.; Meijer, E. W. *Chem. Eur. J.* **1998**, *4*, 2456−2466.

Scheme 4. Synthetic Route to the Laterally Attached Mesogenic Unit L[a]

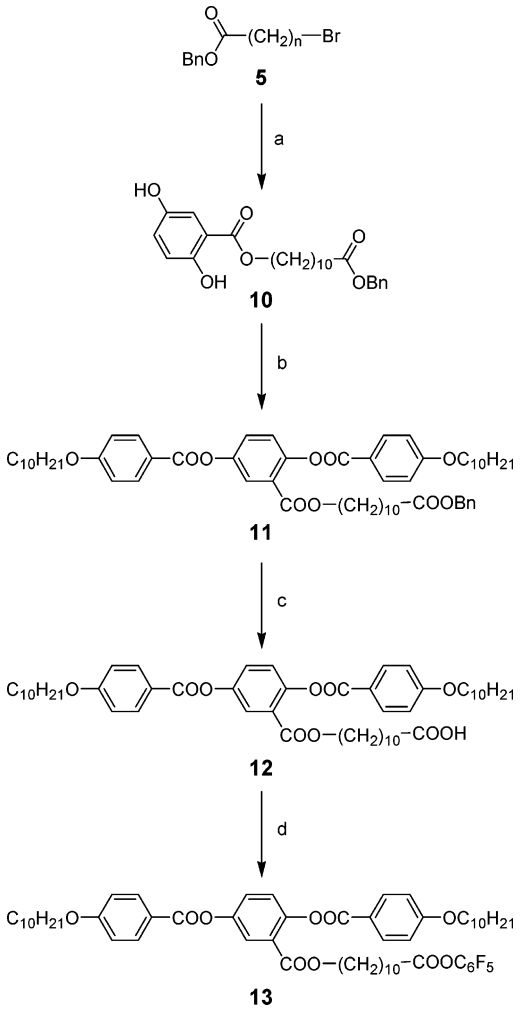

[a] Conditions: (a) $NaHCO_3$, 2,5-dihydroxybenzoic acid, DMF;[32] (b) 4-decyloxybenzoic acid, DCC, DMAP, CH_2Cl_2;[31] (c) $Pd(OH)_2/C$ (20%), cyclohexene, THF; (d) C_6F_5OH, DCC, DMAP, CH_2Cl_2.[31]

attached promesogenic units are statistically distributed around the dendrimer core, essentially due to their similar reactivity with the dendritic core, both in terms of position and number as determined by the initial ratio of L/T or T*. The compounds are in general soluble in dichloromethane and chloroform, partially soluble in THF, and insoluble in ethanol.

Characterization. The chemical structures of the codendrimers were established on the basis of ^1H and ^{13}C NMR and IR spectroscopies and elemental analysis. All of these techniques gave satisfactory results. Fortunately, most of these materials are very soluble in chloroform, except for DL_8T_{24} and DT_{32}, for which a good ^{13}C NMR spectrum could not be recorded due to their low solubility at room temperature.

IR and ^1H and ^{13}C NMR spectroscopic techniques have proved to be very useful in determining the structure and the purity of these materials. The complete amide bond formation was confirmed up to the technique sensitivity by the lack in the ^1H and ^{13}C NMR spectra of signals at $\delta = 2.62$ and $\delta = 41$ ppm, respectively corresponding to the methylene unit α to the primary amine groups of the starting dendrimer.

Table 1. Experimental %L Obtained from the Integration of NMR Spectra of the Reported Codendrimers

		% L_{exp}	
compound	% L_{theor}	^1H NMR	^{13}C NMR
$DL_{24}T^*_8$	75	71	68
$DL_{16}T^*_{16}$	50	48	45
$DL_{12.8}T^*_{19.2}$	40	36	33
$DL_{10}T^*_{22}$	31	27	28
$DL_8T^*_{24}$	25	20	23
$DL_{24}T_8$	75	76	73
$DL_{19.2}T_{12.8}$	60	53	52
$DL_{18}T_{14}$	56	49	49
$DL_{16}T_{16}$	50	46	51
DL_8T_{24}	25	20	–

These results are in agreement with the negative ninhydrine test obtained for these materials.

Due to the synthetic method, the ratio between the number of the laterally and the terminally attached mesogenic units in each molecule was statistical. The average ratio in the material was experimentally determined by the use of NMR techniques.

The most useful technique to obtain this ratio was ^{13}C NMR, because of its better resolution compared to ^1H NMR. As reported above, only in a few cases good enough spectra could not be obtained.

Two pairs of sets of signals corresponding to chemically similar aromatic carbons, the same for all the series, were selected. In Figure 1, we present the correspondence of the selected ^{13}C and ^1H NMR signals with the mesogenic units employed.

For ^1H NMR there are no limitations when comparing the integrals of chemically different proton signals. In Figure 2, we show the evolution of the selected proton signals when the ratio L/T* or T increases. With this technique the choice of the peaks to be compared was necessarily different for both the chiral and achiral series. For T, only the aromatic peaks were taken into account, since $ArOCH_2CH_2$ exhibits an identical chemical shift for L and T. The peak correspondences are presented in Figure 1, and the results are collected in Table 1.

As can be seen, there is a good agreement between the experimental and theoretical values. However, the promesogenic units T and T* seem to be slightly more reactive for amide bond formation, as demonstrated by an experimental percentage of L smaller than that expected.

GPC chromatograms obtained for each compound of the series confirm this statistical distribution of the codendrimers by exhibiting broad peaks containing a maximum centered on the desired compound. However, good polydispersities were obtained. As is usual when working with dendrimers, the molecular masses are underestimated with this technique, since the polystyrene standards used for calibration consist of linear polymers, which are very different from the dendrimers.

To determine accurately the molecular weight distribution of these materials, MALDI experiments were carried out. The data are collected in Table 2. The molecular weights measured with this technique were smaller but very close to those expected. A few amino groups of the parent dendrimer may remain unreacted due to steric reasons, which also may prevent their detection with chemical reactives such as ninhydrine. Furthermore, the data obtained from MALDI are only

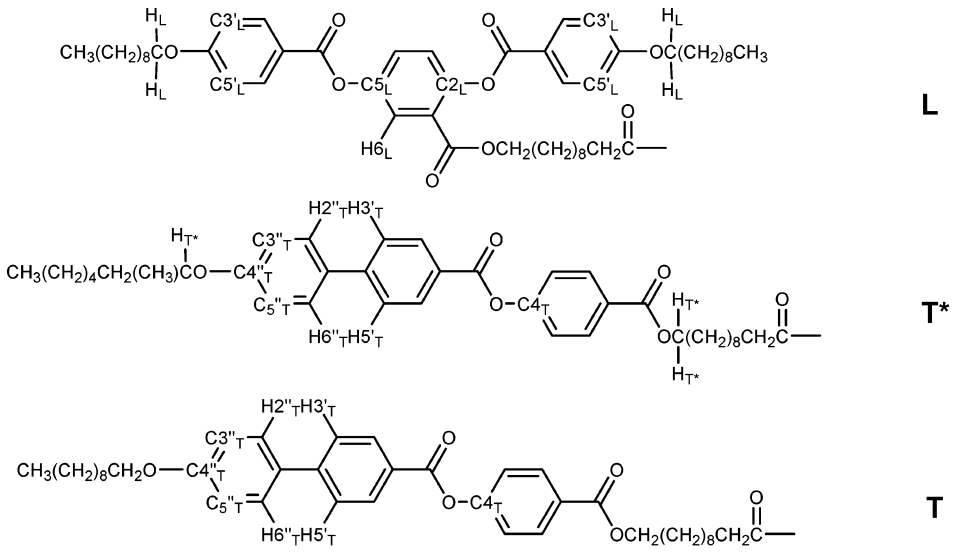

Signal	δ (ppm)	Number of protons or carbons in the promesogenic unit
H_L	3.98; 4.08	6H
H_{T*}	4.25; 4.40	3H
$H6_L$	7.84	1H
$H2''_T$, $H6''_T$, $H3'_T$,$H5'_T$	7.53; 7.63	4H
$C3'_L$, $C5'_L$	114.3; 114.4	2C
$C3''_T$, $C5''_T$	116.2	2C
$C2_L$, $C5_L$	148.1; 148.3	2C
$C4''_T$, $C4_T$	154.6; 158.7	2C

Figure 1. NMR peaks used to find the experimental percentage of L in the reported materials.

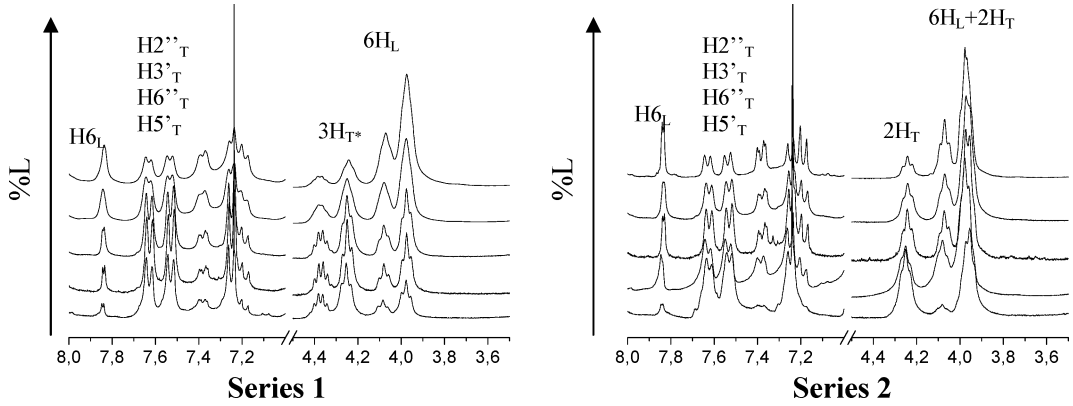

Figure 2. Evolution of the selected ^{1}H NMR signals when varying the L/T* (or T) ratio.

completely reliable for sufficiently low polydispersities.[33] The higher molar mass species require higher laser power for the desorption/ionization process, giving less intense peaks for the high component. Moreover, the lower detection efficiency for bigger ions also plays a role. Thus, for samples with higher polydispersity as in the case of these codendrimers with polydispersities higher than 1.10, MALDI-TOF detects only the lower mass fraction of the distribution.

Mesogenic Behavior. The liquid crystalline properties of these compounds were studied by polarizing optical microscopy (POM) and differential scanning calorimetry (DSC) and confirmed by X-ray diffraction (XRD).

Polarizing optical microscopy (POM) allowed us to identify three general types of mesogenic behavior within both series of codendrimers. First, those with a higher proportion of the laterally attached mesogenic units gave a nematic texture. In the case of the chiral

(30) Mitsunobu, O. *Synthesis* **1981**, 1−28.
(31) Hassner, A.; Alexanian, V. *Tetrahedron Lett.* **1978**, 4475−4478.
(32) Keller, P.; Thomsen, D. L., III; Li, M.-H. *Macromolecules* **2002**, *35*, 581−584.
(33) Pasch, H.; Schrepp, W. *MALDI-TOF Mass Spectrometry of Synthetic Polymers;* Springer-Verlag: Berlin, 2003; Chapters 3 and 5.

Table 2. GPC and MALDI TOF Data for the Reported Codendrimers

	GPC results					MALDI-TOF results			
codendrimer	$M_{w\ theor}$	M_n	M_w	I	$M_n/M_{w\ theor}$	M_n	M_w	I	$M_n/M_{w\ theor}$
DT^*_{32}	23 123	13 570	13 931	1.03	0.59	19 161	20 392	1.06	0.83
$DL_8T^*_{24}$	24 974	11 557	14 380	1.24	0.46	22 630	23 300	1.03	0.93
$DL_{10}T^*_{22}$	25 407	14 828	17 147	1.16	0.58	23 091	23 843	1.03	0.91
$DL_{12.8}T^*_{19.2}$	26 046	13 212	15 565	1.18	0.51	21 825	22 676	1.04	0.84
$DL_{16}T^*_{16}$	26 776	16 558	20 230	1.22	0.62	23 675	24 554	1.03	0.88
$DL_{24}T^*_8$	28 603	16 355	18 773	1.15	0.57	26 295	26 907	1.02	0.92
DT_{32}	24 021	–	–	–	–	26 288	27 432	1.04	1.09
DL_8T_{24}	25 623	–	–	–	–	21 495	22 376	1.04	0.84
$DL_{16}T_{16}$	27 225	17 741	19 736	1.11	0.65	25 048	25 754	1.03	0.92
$DL_{18}T14$	27 606	16 232	18 609	1.15	0.59	24 046	24 786	1.03	0.87
$DL_{19.2}T_{12.8}$	27 866	14 773	17 117	1.16	0.53	25 269	25 690	1.02	0.91
$DL_{24}T_8$	28 828	17 546	19 947	1.14	0.61	26 796	27 432	1.02	0.95

Table 3. Thermal (°C) and Thermodynamic (ΔH/kJ mol^{-1}, in parentheses) Data for the Phase Transitions Observed on Cooling the Codendrimers Belonging to the Chiral Series[a]

	C	SmC̃	SmÃ	SmC*	SmA	N(*)	I
DL_{32}		• 36 (81)				• 65 (33)	•
$DL_{24}T^*_8$		• 25 (38)				• 70 (50)	•
$DL_{16}T^*_{16}$			• 57 (216)			• 90 (15)	•
$DL_{12.8}T^*_{19.2}$	• 62 (399)			• 106 (48)			•
$DL_{10}T^*_{22}$	• 64 (391)				• 109 (41)		•
$DL_8T^*_{24}$	• 78 (450)				• 115 (30)		•
DT^*_{32}	• 88 (592)				• 116 (44)		•

[a] g = glass; C = crystal; SmC̃ = modulated smectic C phase; SmÃ = modulated smectic A phase; SmC* = chiral smectic C mesophase; SmA = smectic A mesophase; N(*) = nematic or chiral nematic mesophases; I = isotropic liquid.

series (series 1), though a color change of the texture was observed as the temperature was varied, textures were not those typically described for chiral nematic phases.[34] Thus, POM observations were not enough to elucidate whether the mesophase was chiral or not. Circular dichroism (CD) studies were performed and confirmed the chiral nematic mesophase. It is important to note that the chirality of the mesophase is already obtained, for a low percentage of chiral promesogenic unit as occurs in low molecular weight liquid crystals.

When the terminally attached mesogenic unit is predominant, the transition temperatures increase. In the mesophase, the materials exhibit fan-shaped and homeotropic textures, characteristic of a smectic A mesophase. Upon cooling, the materials either retained their texture or exhibited a clear crystallization.

For the intermediate proportions, a lamellar behavior was also observed, but in these cases no homeotropic domains could be obtained in a temperature range revealing that the mesophase was smectic C.

Finally, a decrease in the viscosity of the mesophase could be observed qualitatively in the POM studies as the amount of L increased. This fact allowed us to think that the ferroelectric properties could be measured in the appropiate codendrimers of series 1.

Differential Scanning Calorimetry (DSC). The optical, thermal, and thermodynamic data of the dendrimers of series 1 and series 2 are gathered in Tables 3 and 4, respectively.

After the observation of the DSC curves, two groups of codendrimers can be distinguished in series 1.

Table 4. Thermal (°C) and Thermodynamic (ΔH/kJ mol^{-1}, in parentheses) Data for the Phase Transitions Corresponding to the First Cooling Scan of the DSC for the Codendrimers Belonging to the Achiral Series (series 2)[a]

	C	SmC̃	SmC	SmA	N	I
DL_{32}		• 36 (81)			• 64 (34)	•
$DL_{24}T_8$		•[b]			• 82 (20)	•
$DL_{19.2}T_{12.8}$	• 72 (138)		• 102	• 113 (7)		•
$DL_{18}T_{14}$	• 69 (253)		• 106	• 119 (78)		•
$DL_{16}T_{16}$	• 73 (242)			• 115 (26)		•
DL_8T_{24}	• 67 (149)			•[c] 125-130		•
DT_{32}	• 78 (270)			•[c] 140-145		•

[a] g = glass; C = crystal; SmC̃ = modulated smectic C phase; SmC = smectic C mesophase; SmA = smectic A mesophase; N = nematic mesophase; I = isotropic liquid. [b] Transition detected only by XRD studies. [c] Transition detected by POM and XRD studies. The temperatures for the appearance of the texture are given.

$DL_{24}T^*_8$ exhibits a behavior very similar to that of the same generation homodendrimer with 32 laterally grafted mesogens that some of us described previously.[15] Thus, there is a broad crystal to isotropic liquid transition in the first heating and two first-order transitions on the other cycles, one of them corresponding to the clearing point and the other one to a phase transition between a chiral nematic mesophase and a low-temperature mesophase. This transition was not detected by POM, but the low-temperature mesophase was identified by XRD studies as a modulated smectic C mesophase (SmC̃).

(34) Demus, D.; Richter, L. *Textures of Liquid Crystals;* Verlag Chemie: Weinheim, 1978; pp 49−61.

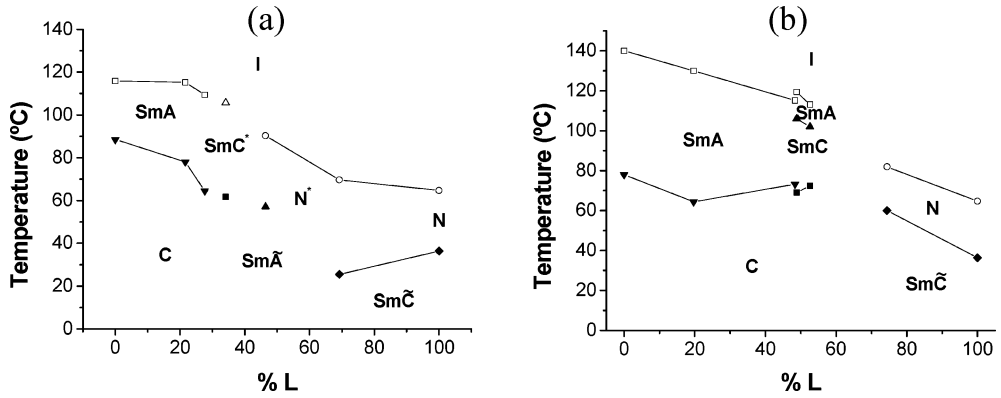

Figure 3. Second cooling DSC data for the $DL_xT^*_{(32-x)}$ series (a) and for the $DL_xT_{(32-x)}$ series (b).

The other codendrimers of series 1 exhibit a different behavior. After a first heating scan to eliminate the thermal history of the material, the cooling process shows two transition peaks. The higher temperature peak corresponds to an isotropic liquid to mesophase transition and the lower one to a nematic to another mesophase transition in the case of $DL_{16}T^*_{16}$ and a crystallization in all the others. In the subsequent heating scans, all of the DSC curves exhibit a very broad transition from the low-temperature phase to the isotropic liquid. Despite this, in all the materials there is a mesophase interval observed by POM in the heating scan which is not detected by DSC because the weak clearing point peak might be hidden under the much more endothermic melting peak. For this reason, only the data corresponding to the cooling scan are gathered in Table 3.

It is noticeable that when the amount of T* is higher than 50%, the transition temperatures observed in the cooling scans decrease as the material undergoes more cycles. This could be a consequence of the higher viscosity of these codendrimers as the amount of T* increases, as shown by the broad peaks in the DSC thermograms. Thus, a rapid arrangement to the most stable organization is hindered and certain degree of order is lost in each cycle.

As may be observed, the transitional enthalpy for the chiral nematic to the lower temperature mesophase of $DL_{16}T^*_{16}$ is about 6 times higher than that of $DL_{24}T^*_8$. Although the POM textures are very similar for both materials, the low-temperature mesophase is different, as XRD studies finally confirm.

After considering the data in Table 3, some trends can be immediately deduced. First, there is a gradual evolution from nematic to lamellar behavior when increasing the proportion of terminally attached mesogenic units. At the same time, the transition temperatures increase accordingly. The enthalpies of crystallization also increase in the group of codendrimers with a higher proportion of T*. When comparing the homodendrimer DL_{32} with the codendrimer $DL_{24}T^*_8$, the nematic mesophase gains stability when T* is incorporated, since it hinders the modulated smectic phase favored by L at lower temperatures. The end-on attachment facilitates the molecular packing and increases the interaction between the mesogenic cores.

For the achiral series (series 2), the DSC peaks were sometimes even 30 or 40 °C wide and not intense. Thus, the data we provide for this series come from the peak maxima rather than from the peak onset and the temperatures observed by POM are higher. As for series 1, the broad melting peak prevents the detection of a mesophase range by DSC in the heating scans, which is actually observed by POM. Therefore, only the thermal and thermodynamic data for the cooling scans are gathered in Table 4.

The nematic $DL_{24}(T_{10})_8$ exhibits a wide melting peak in the first heating scan and a wide mesophase to isotropic transition at a higher temperature. In the next cycles, only the nematic to isotropic liquid transition is observed. However, another mesophase is detected at lower temperatures by XRD. The other codendrimers of the series, which exhibit smectic behavior, undergo a wide melting transition upon heating, but no mesophase to isotropic liquid transition is observed. Upon cooling, apparently there is a very broad isotropic liquid to mesophase transition peak. The crystallization is slow, so the peak is broad, but the high enthalpy allows its detection. As observed in the chiral series, the transition temperatures in the cooling scans decrease progressively as the number of cycles increases.

Essentially the same trends as for series 1 can be deduced here; however, the transition enthalpies do not follow a regular trend. As was mentioned previously, the DSC curves are difficult to interpret for this series.

In Figure 3, we present an overview of the mesogenic behavior of the codendrimers. When comparing both series, the transition temperatures for the first are lower than those of second, due to the lack of a branch in the terminal chain of T in series 2. This branch, very close to the mesogenic core, hinders the parallel packing of the mesogenic units. This is also the explanation for the faster appearance of the nematic behavior in series 1. It is noticeable that the evolution from nematic behavior to a more ordered smectic A behavior occurs through a smectic C mesophase in both series, when a more disordered arrangement should be expected from a mixture of such different mesogenic units. For both series, the flexibility of the long spacer between the mesogenic moieties and the dendritic matrix as well as the flexibility of the dendritic matrix itself must be the keys to reach this more stable mesophase.

X-ray Diffraction Studies. The data obtained by XRD studies are collected in Table 5 for series 1 and 2.

For a clearer description of the XRD results, the codendrimers are divided into two groups. The first includes all the codendrimers that exhibit nematic behavior, irrespective of whether they are chiral ne-

Table 5. X-ray Data for the Mesophases of the Codendrimers in the Chiral and Achiral Series[a]

compound	mesophase	T (°C)	d_1 (Å)	d_2 (Å)
		Chiral Series		
DL_{32}	N	50	35 (diffuse)	–
	SmC̃	rt	33.6	21.4
$DL_{24}T^*_8$	N	68	30.4 (diffuse)	–
	SmC̃	rt	36.6	22.8
$DL_{16}T^*_{16}$	N	90	25.0 (diffuse)	–
	SmÃ	rt	41.4	25.7
$DL_{12.8}T^*_{19.2}$	Sm	103	55.2	–
$DL_{10}T^*_{22}$	Sm	95	56.3	–
DL_8T_{24}	Sm	110	53.4	–
DT^*_{32}	Sm	125	54.1	–
		Achiral Series		
DL_{32}	N	50	35 (diffuse)	–
	SmC̃	rt	33.6	21.4
$DL_{24}T_8$	N	79	33 (diffuse)	–
	SmC̃	rt	38.8	22.5
$DL_{18}T_{14}$	Sm	rt	56.9	–
$DL_{16}T_{16}$	Sm	124	54.1	27.1
DL_8T_{24}	Sm	134	53.4	–
DT_{32}	Sm	rt	60.8	31.4

[a] Parameters d_1 and d_2 are the two observed Bragg spacings.

matic, or not. The other codendrimers, which exhibit lamellar mesomorphism, will be classified in a second group.

The nematic nature of the high-temperature mesophase found in the codendrimers of the first group was demonstrated by XRD. In all the cases, the powder diffraction pattern consists of two diffuse halos, one of which is in the small-angle region and the other in the wide-angle region. No oriented samples were studied, but the assignment of the mesophase is unambiguous on the basis of XRD and POM studies.

In agreement with the existence of a DSC peak in the cooling scans at the lower temperature limit of the nematic mesophase, the X-ray experiments revealed the existence of an additional LC phase below the nematic mesophase for all the compounds of this group.

The patterns obtained from unoriented samples consist of two sharp rings in the small-angle region and a diffuse halo in the wide-angle region. The ratio between the spacings corresponding to the two small-angle region maxima is neither in the reciprocal ratio 1:2 nor in the reciprocal ratio $1:\sqrt{3}$, which would indicate a simple lamellar structure or a hexagonal structure, respectively. Therefore, a lamellar mesophase with a ribbonlike structure was proposed (also called a "modulated"smectic).[35]

With the aim of verifying this hypothesis, X-ray patterns were obtained from mechanically aligned samples (Figure 4). For $DL_{24}T^*_8$ and $DL_{24}T_8$, the patterns are qualitatively identical to those of the homodendrimer. The diffuse crescents centered on the equator indicate that the molecules are oriented in the stretching direction. Each of the low-angle maxima condense into an off-meridian four-point pattern, which indicates that these maxima correspond to long-range correlations that are neither in the meridional nor in the equatorial direction. Furthermore, the two spots observed in each quadrant are not in the same direction (the azimuthal angles of the two sets of maxima are not the same). These facts are consistent with the ribbonlike smectic structure reported in the literature for other kinds of liquid crystals.[35]

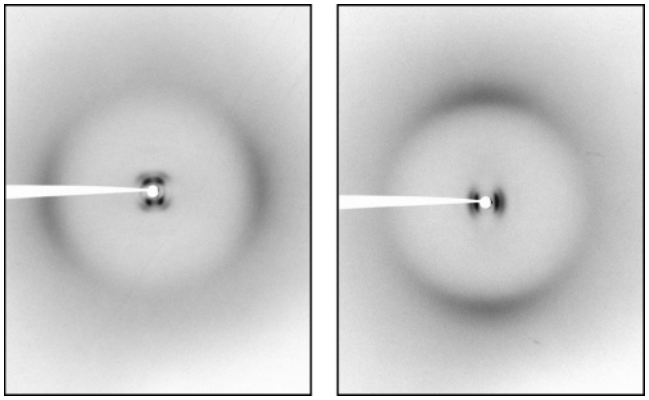

Figure 4. (Left) XRD pattern of the low-temperature mesophase of $DL_{24}T^*_8$, which is assigned as SmC̃. The mesogenic units are oriented vertically. (Right) XRD pattern of the low-temperature mesophase of $DL_{16}T^*_{16}$. Shearing in the vertical direction oriented the mesophase.

In contrast, the diffraction patterns of oriented samples of $DL_{16}T^*_{16}$ reveal that a different kind of mesophase occurs. First, the diffuse crescents parallel to the equator in the wide-angle region reveal that the molecules are oriented approximately perpendicular to the shearing direction. Thus, assuming a lamellar behavior, the layers are oriented in the stretching direction. This kind of orientation is analogous to that of the classic smectic mesophases of LC dendrimers that we have described previously. Each maximum in the small-angle region condenses into two crescents centered in the equatorial direction, which might be a poorly resolved off-meridian four-point pattern. These data are consistent with a modulated smectic A mesophase (SmÃ).

In the second group of codendrimers, the lamellar behavior was unambiguously confirmed by the X-ray diffraction studies. The diffractograms obtained from unoriented samples consist of a diffuse halo in the wide-angle region and a set of two maxima in the small-angle region, with spacings in the reciprocal ratio of 1:2. This pattern is consistent with the lamellar behavior observed by POM. Since the maxima were not sufficiently sharp, it was not possible to study carefully how the layer spacing varies both with temperature and composition. In some cases, the maximum corresponding to the first-order reflection was somehow diffuse and too close to the beam-stop to be taken into account. From the available data we can confirm the bilayer model for the classical smectic mesophases of these materials, since the layer spacings are comparable to others we have obtained previously with other derivatives of the fourth-generation poly(propyleneimine) dendrimer.[2]

Ferroelectric Properties. Despite favoring SmC* mesomorphism, the codendrimer $DL_{12,8}T^*_{19,2}$ exhibits poor ferroelectric properties. The material could be introduced by capillarity in a commercial cell with ITO electrodes. Unfortunately, no switching was observed even at very high voltages (500 V_{pp}) in the SmC* mesophase temperature range. Moreover, this high voltage produced the apparent decomposition of the material. The use of DAB derivatives appears to produce dendrimers with very high viscosities, and hence mo-

(35) Seddon, J. M. *Handbook of Liquid Crystals*; Demus, D., Goodby, J. W., Gray, G. W., Spies, H. W., Vill, V., Eds.; VCH: Weinheim, 1998; Vol. 1, pp 656–657 and references therein.

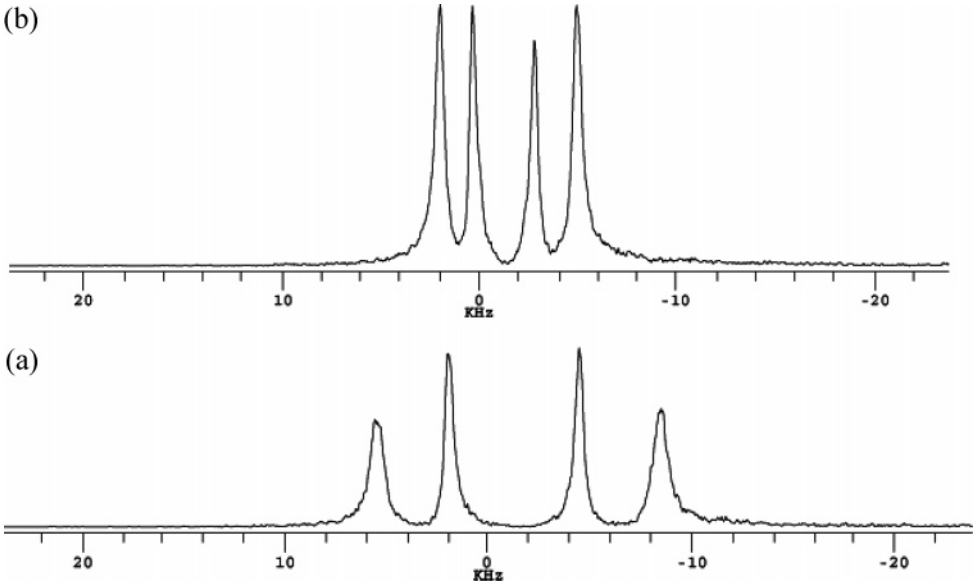

Figure 5. Deuterium NMR spectra of 2.5 wt % *p*-xylene-d_{10} dissolved in the codendrimer $DL_{24}T_8$ at 65.0 °C (a) before rotation and (b) after rotation by 90° from being parallel to the magnetic field.

lecular movement in these systems is extremely difficult. The synthesis of codendrimers to lower the viscosity of this kind of materials seems to be insufficient to permit the appearance of ferroelectric properties in DAB derivatives, and other strategies might be more convenient.

Determination of the Symmetry for the Nematic Phase of Dendrimer $DL_{24}T_8$. Here, we shall consider the determination of the nematic phase exhibited by the codendrimer of series 2, $DL_{24}T_8$ (see Scheme 2). In fact, the unambiguous assignment of the phase symmetry is a difficult task,[36] so a description in some detail of the background to the NMR measurements we have made is provided as Supporting Information.

In our experiments it did not prove possible to deuterate the liquid crystal dendrimer specifically, so it was doped with perdeuterated *p*-xylene-d_{10}. This probe was chosen because previous studies of a highly biaxial crystal E phase had shown that the quadrupolar tensors for both the aromatic and aliphatic deuterons were also strongly biaxial.[37] In addition, because there are two kinds of deuteron in the probe molecule, it is likely that one of them will have a significant biaxiality in the quadrupolar tensor. The deuterium NMR spectrum of the dendrimer doped with *p*-xylene-d_{10} is shown in Figure 5a. It contains two well-resolved quadrupolar doublets, showing that one of the directors has been aligned by the magnetic field of the NMR spectrometer and that the quality of the alignment is good. The splittings can be assigned to the specific groups of deuterons from the integrated intensities of the spectral peaks. These reveal that the smaller splitting comes from the aromatic deuterons and that the larger splitting comes from the aliphatic deuterons. This assignment is consistent with that found for *p*-xylene-d_{10} dissolved in conventional monomeric nematics.[38] The sample was then rotated through 90° and the spectrum was measured immediately. The resultant spectrum is shown in Figure 5b, and we can see that it also contains two quadrupolar doublets but with smaller splittings and smaller line widths. The fact that the spectrum contains just two doublets shows that only one director is aligned parallel to the magnetic field, and the narrowness of the lines again indicates the good alignment of this director. As is explained in the Supporting Information, if the field had been in the plane defined by the two directors, **l** and **m**, then the spectrum would have contained four quadrupolar doublets with splittings determined by the *x* and *y* principal components of the quadrupolar tensors. They would, however, have been broadened because the **l** and **m** directors would have adopted a range of orientations with respect to the magnetic field. If the nematic phase is biaxial, then the observation of just four sharp lines would indicate that one of the minor directors had been rapidly aligned parallel to the field. To place a time scale on the alignment process, we note that the time taken to rotate the sample by 90° and then record the spectrum is approximately 150 s. In this time the major director remains orthogonal to the magnetic field, indicating the high viscosity of the nematic phase. It appears to be unnecessary, therefore, to realign the main director by rotating the sample back through 90° as done for the lyotropic biaxial nematic.[39] The symmetry of the nematic phase formed by the dendrimer can now be determined from the quadrupolar splittings measured for the sample with the main director, **n**, parallel and perpendicular to the magnetic field. For a uniaxial phase, because the quadrupolar tensor is traceless, $q_\perp$ is $-q_\parallel/2$, although the sign of the splitting is not directly available from the NMR spectrum. The values of these tensor components determined from the splittings will depend on how accurately the director is aligned with respect to the magnetic field. When the director is aligned by the field, then clearly the angle that it makes

(36) Galerne, Y. *Mol. Cryst. Liq. Cryst.* **1998**, *323*, 211−229.
(37) Yu, L. J.; Saupe, A. *Phys. Rev. Lett.* **1980**, *45*, 1000−1003.
(38) Dabrowksi, R.; Luckhurst, G. R.; Mainal, R.; Timimi, B. A. Manuscript in preparation.
(39) Emsley, J. W.; Luckhurst, G. R.; Sachdev, H. S. *Liq. Cryst.* **1989**, *5*, 953−967.

with the field is accurately zero. The angle made after rotation is determined by the accuracy of the goniometer, which we judge to be ±2°. The error produced in the splitting by this error in the angle proves to be very small when the angle is approximately 90°. This follows because the splitting is related to the angle between the field and the director by

$$\Delta\upsilon(\beta) = \Delta\upsilon_0 P_2(\cos\beta) \quad (1)$$

where $\Delta\upsilon_0$ is the splitting when the field is parallel to the director and $P_2(\cos\beta)$ is the second Legendre function.[40] It follows from this that for small variations, $\delta\beta$, in β the quadrupolar splitting will have an associated error, $\delta\Delta\upsilon$, given by

$$\delta\Delta\upsilon(\beta) = (3/2)\Delta\upsilon_0 \sin 2\beta\, \delta\beta \quad (2)$$

This means that, in the linear regime, any error in setting the angle in the vicinity of 90° should produce a negligible error in the quadrupolar splitting. The experimental value for the ratio of the splittings for the aliphatic deuterons is 2.03 and 2.10 for the aromatic deuterons. The average of these two is 2.06 ± 0.03, which is certainly within the experimental error of the value expected for a phase with uniaxial symmetry. The experiment was repeated at the lower temperature of 55 °C, and here the average ratio was determined to be 2.00 ± 0.03, again in keeping with the assignment of the nematic phase of the codendrimer $DL_{24}T_8$ as uniaxial.

Orientational Order. The primary purpose of the deuterium NMR experiments was to determine the symmetry of the nematic phase formed by the codendrimer $DL_{24}T_8$. However, the experiments also provide the quadrupolar splittings for the methyl and aromatic deuterons of the probe molecule, *p*-xylene-d_{10}. These splittings are proportional to the principal components of the Saupe ordering matrix for *p*-xylene-d_{10}, and these in turn are related to the orientational order of the nematic host.[38] It is of interest, therefore, to compare the quadrupolar splittings for the probe dissolved in the dendritic host with those determined for a conventional, monomeric nematic. The two quadrupolar splittings are shown in Figure 6 for *p*-xylene-d_{10} in the dendritic host as a function of the shifted temperature ($T_{NI} - T$). The results show that the two splittings jump from zero in the isotropic phase and then increase, albeit slowly, with decreasing temperature in the nematic phase. However, at a shifted temperature of about 25 °C, corresponding to the formation of the smectic C phase, the splittings decrease and then remain essentially constant. This behavior is consistent with the exclusion of the probe molecule from the more to the less ordered regions of the smectic phase. For comparison we also show, in Figure 6, the quadrupolar splittings measured for *p*-xylene-d_{10} dissolved in the nematogen I22 (Merck Ltd.), which is 1-(*trans*-ethylcyclohexyl)-2-(2′-fluoro,4′-ethyl,4-biphenyl)ethane and has a low polarity. The splittings are seen to exhibit a more or less continuous increase with decreasing temperature following the transition to the nematic phase. The aromatic splittings

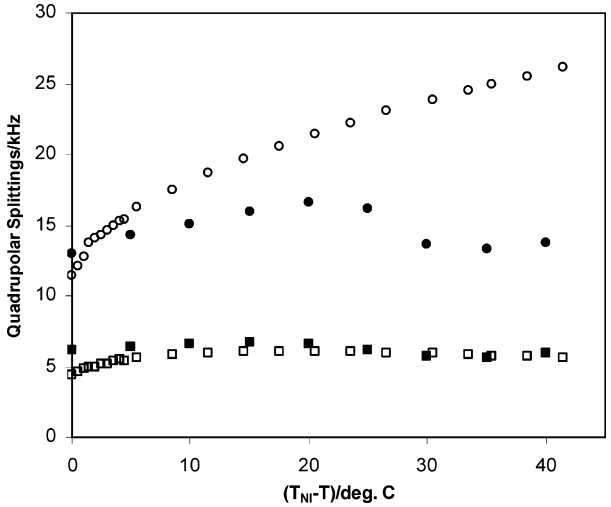

Figure 6. The dependence of the quadrupolar splittings for *p*-xylene-d_{10} dissolved in $DL_{24}T_8$ [methyl (■), aromatic (●)] and I22 [methyl (□), aromatic (○)].

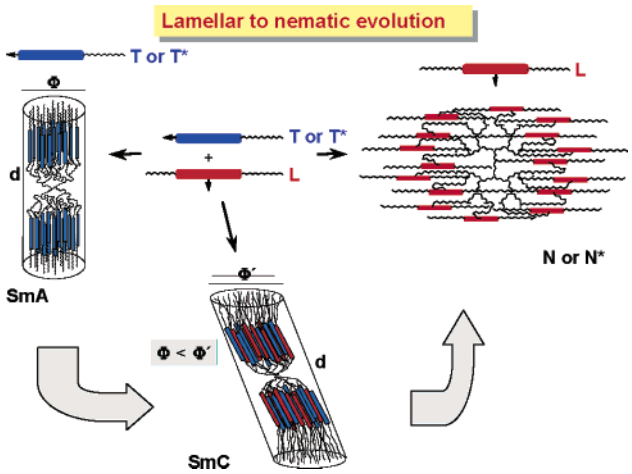

Figure 7. Lamellar to nematic evolution as a function of the number of promesogenic units L and T or T*.

are seen to be very similar for both the codendrimer and I22, although the splitting for I22 varies more rapidly with temperature than for the codendrimer.

This difference is more apparent for the methyl splittings where, although comparable near the nematic−isotropic transition, at lower temperatures the difference increases and at the lowest shifted temperatures the aromatic splitting for I22 is significantly larger than for the codendrimer. However, part of this difference must be attributed to the existence of the smectic C phase for the codendrimer. Nonetheless, it is apparent that the orientational ordering in the codendrimer and monomer are similar, despite the dramatic difference in the architecture of the two mesogenic groups.

Conclusions

In this paper we have presented two novel series of codendrimers as a way to improve the properties of the homodendrimers. First, as a consequence of the introduction of laterally and terminally attached mesogenic units, the appearance of a smectic C mesophase has been promoted; this was not exhibited by the homodendrimers. Thus, the "new" mesophase that the intermediate codendrimers present is surprisingly more ordered

(40) Hughes, J. R.; Kothe, G.; Luckhurst, G. R.; Malthete, J.; Neubert, M. E.; Shenouda, I.; Timimi, B. A.; Tittlebach, M. *J. Chem. Phys.* **1997**, *107*, 9252−9263.

than those of the homodendrimers, which is an apparent contradiction, but that could be explained by the flexibility of the dendritic matrix and the long spacer of the promesogenic units. Unfortunately, the chiral smectic mesophases obtained in series 1 did not exhibit any ferroelectric switching, even at high voltages.

Therefore, this study has enabled us to confirm that the mesomorphic behavior of such block molecules could be modulated and controlled by a simple modification of the ratio of two promesogenic units present around the dendrimer core (Figure 7). ^{2}H NMR experiments carried out on one of these codendrimers have proved that the symmetry of the nematic phase is uniaxial, in contrast to the biaxial nematic phase observed for some side-on polymers in the literature.[22]

Acknowledgment. This work has been supported by the CICYT of Spain (MAT 2002-04118-C02-01 and MAT 2003-07806-C01) and FEDER (EU). We also thank Dr. Joaquín Barberá (Universidad de Zaragoza) for help with X-rays studies. R.M. acknowledges a fellowship from MECD (Spain). G.R.L. thanks the Higher Education Funding Council for England for the award of a grant (JR00SOLEEQ) under the 2000 JREI to cover the cost of the Varian NMR spectrometer. A.M. acknowledges the Government of Malaysia and the University Malaya (Malaysia) for the award of a Scholarship.

Supporting Information Available: Experimental section containing techniques, the synthesis and analytical data of all the codendrimers, and background to the NMR measurements of the biaxiality nematic phase. This material is available free of charge via the Internet at http://pubs.acs.org.

CM049191L